Available online at www.sciencedirect.com

ScienceDirect

Geochimica et Cosmochimica Acta 293 (2021) 365–378

Geochimica et Cosmochimica Acta

www.elsevier.com/locate/gca

An isotopic study of abiotic nitrite oxidation by ligand-bound manganese (III)

Jennifer S. Karolewski [a,b], Kevin M. Sutherland [a,b,1], Colleen M. Hansel [a], Scott D. Wankel [a,*]

[a] Department of Marine Chemistry and Geochemistry, Woods Hole Oceanographic Institution, Woods Hole, MA 02540, United States
[b] Department of Earth, Atmospheric and Planetary Sciences, Massachusetts Institute of Technology, Cambridge, MA 02139, United States

Received 18 May 2020; accepted in revised form 3 November 2020; available online 13 November 2020

Abstract

Redox transformations of nitrogen (N) play a critical role in determining its speciation and biological availability, thus defining the magnitude and extent of productivity in many ecosystems. A range of important nitrogen transformations often co-occur in regions hosting other redox-active elements, including sulfur, iron, and manganese (Mn), especially along sharp redox gradients within aquatic sediments. This proximity in "redox real estate" produces conditions under which multi-element interactions and coupled cycling are thermodynamically favored. While previous work has reported anoxic nitrification linked to the presence of manganese (Mn) oxides in sediments, a clear connection between the cycling of Mn and N has remained elusive. Soluble Mn(III), which is stabilized via ligand-complexation, has recently been shown to represent the dominant dissolved Mn species in many environments. Here, we examined the reactivity of ligand-stabilized Mn(III) with nitrite, using natural abundance stable nitrogen and oxygen isotopes to explore reaction dynamics under a range of conditions. Oxidation of nitrite to nitrate by Mn(III)-pyrophosphate proceeded abiotically under both oxygen replete and nitrogen-purged conditions. Kinetics and isotope systematics of this reaction were measured over a range of pH (5–8), with reaction rates decreasing with increasing pH. Under all treatments, an inverse kinetic isotope effect of -19.9 ± 0.7‰ was observed for N, remarkably similar to previously documented fractionation by nitrite-oxidizing organisms. Experiments using ^{18}O-labeled water confirmed that the source of the additional oxygen atom was from water. These findings suggest that nitrite oxidation in environments hosting abundant ligand-bound Mn(III), including porewaters, estuaries, and coastal waters, may be facilitated in part by abiotic reactions with Mn, even under functionally anoxic conditions.

Keywords: Nitrogen isotopes; Oxygen isotopes; Nitrite; Nitrate; Manganese; Ligand-bound manganese; Mn(III); Inverse isotope effect; Anoxic nitrification; Anoxic nitrite oxidation

1. INTRODUCTION

As a primary nutrient for sustaining life, nitrogen (N) and the processes governing its transformations have long been a topic of interest. The N cycle is also intricately linked with the cycling of other important elements in aquatic environments, including carbon, oxygen, phosphorous, sulfur, iron, and manganese (Mn) (Burgin et al., 2011; Gruber and Galloway, 2008; Melton et al., 2014). While

* Corresponding author.
E-mail address: sdwankel@whoi.edu (S.D. Wankel).
[1] Currently in Department of Earth and Planetary Sciences, Harvard University, Cambridge, MA 02138, United States.

https://doi.org/10.1016/j.gca.2020.11.004
0016-7037/

the cycling of nitrogen has traditionally been attributed to microbially-mediated transformations, recent studies have highlighted abiotic processes as likely important and understudied aspects of nitrogen cycling under some conditions (Cavazos et al., 2018; Doane, 2017; Heil et al., 2016; Stanton et al., 2018; Zhu-Barker et al., 2015).

Redox interactions between Mn and N in sediments have been the focus of previous studies, however, their importance in global cycling is still poorly understood (Doane, 2017; Zhu-Barker et al., 2015). For example, Luther et al. (1997) showed in laboratory and field studies that reactions between ammonia (NH_3) and Mn(III,IV) (oxy)(hydr)oxides (hereinafter Mn oxides) in sediments could act to "short circuit" the nitrogen cycle by providing a direct pathway to the formation of dinitrogen gas ($2NH_3 + 3MnO_2 + 6H^+ \rightarrow 3Mn^{2+} + N_2 + 6H_2O$). Subsequent work also found indirect evidence for anoxic nitrification coupled to reduction of Mn oxides to Mn(II) (Anschutz et al., 2000; Hulth et al., 1999). In contrast, however, targeted studies using incubations amended with $^{15}NH_4^+$ failed to find conclusive evidence that reactions between ammonia and manganese were occurring in a Mn oxide rich continental basin sediment (Thamdrup and Dalsgaard, 2000). More recent field studies have suggested that the specific geochemical conditions, including the concentration and age of the Mn oxides, are key factors controlling the efficacy of Mn oxide catalyzed anaerobic nitrification (Bartlett et al., 2007, 2008), or that reactions may only occur in presence of colloidal Mn oxides or more reactive Mn(III) species (Luther and Popp, 2002; Lin and Taillefert, 2014).

While many biogeochemical models of Mn in sediments include only soluble Mn(II) and solid Mn(III,IV) oxides, soluble Mn(III) can be stabilized via complexation by ligands and has been recently shown to represent the dominant dissolved Mn species in many environments (Madison et al., 2013; Oldham et al., 2015). With a reduction potential close to that of molecular oxygen (Luther et al., 1997; Luther III, 2010), Mn(III)-ligand (Mn(III)-L) complexes have the capacity to be potent and important environmental oxidants. For instance, Mn(III)-L complexes can directly oxidize carbon, ferrous iron, and sulfide (Kostka et al., 1995). Ultimately, the extent to which Mn(III)-L complexes interact with other redox-active elements and molecules will depend on the specific ligand and subsequent strength of Mn(III) complexation. While the composition of Mn(III) ligands in natural systems is presently unknown, a diversity of ligand compositions and complex strengths has been predicted, ranging from weaker ligands such as pyrophosphate to complex humics with strong ligand moieties (Yakushev et al., 2009; Oldham et al., 2015, 2017a).

The role of Mn(III) in Mn-N redox interactions is a potentially important component in the biogeochemical cycles of both elements that has not been fully addressed by previous studies (Luther et al., 1997, 2018). One major challenge to studying coupled cycling reactions is determining the importance of a single process from a range of potential biotic and abiotic reactions occurring in the environment. Stable isotope studies of nitrogen and oxygen have proven to be powerful tools in decoupling complex processes in the nitrogen cycle across a range of environments and contexts (Kendall et al., 2007; Casciotti, 2016). The abundance ratio of the two stable isotopes of N (^{14}N and ^{15}N) as well as O (^{16}O and ^{18}O) can vary as the result of isotope fractionation during processes including enzymatic or chemical reactions. As specific reactions may yield unique isotopic fractionation patterns, measurements of isotope ratios can be used to disentangle complex processes in the environment (Granger and Wankel, 2016). Hence, a focus of this study is to characterize the isotopic fractionation of specific reactions in order to identify abiotic, anoxic nitrite oxidation by ligand-stabilized Mn(III). Here we hypothesize that Mn(III) is a viable and environmentally relevant oxidant of nitrite (NO_2^-) in aquatic systems. We present a series of experiments describing one such potentially important reaction between Mn(III) and NO_2^-, and provide the first examination of the stable N and O isotope dynamics captured by the reaction.

2. METHODS

2.1. Experimental Overview

Aspects of the reaction between Mn(III) and NO_2^- were targeted through a variety of experimental approaches. Specifically, experiments were conducted to evaluate 1) the influence of reactant concentrations and pH on the reaction kinetic expression, 2) the kinetic nitrogen isotope effect of NO_2^- oxidation by measurement of reactant and product isotopic compositions over reaction progress, 3) the influence of dissolved O_2 on reaction rates by varying solution and headspace composition, 4) the possible role of chemically catalyzed equilibrium (or back-reaction) between NO_2^- and reaction products (by use of NO_3^- with an elevated $\delta^{15}N$), and 5) the source of O atoms in reaction product NO_3^- (by use of ^{18}O-labeled water).

2.2. Preparation of solutions

Manganese(III)-pyrophosphate (Mn(III)-PP) solutions were prepared as previously described (Madison et al., 2011). A 5 mM solution of sodium pyrophosphate was prepared in de-oxygenated milliQ water and the pH adjusted to 7.0 using 6 M hydrochloric acid (HCl). Manganese (III)-acetate salt was added to form a clear pink Mn(III)-PP solution (approximately 1 mM) which was subsequently filtered (0.45 μm) to remove any incidental particulate Mn oxides formed via disproportionation. The pH of Mn (III)-PP was adjusted by addition of 6 M HCl before filter sterilization (0.2 μm). Additional solutions of Mn(III)-PP were prepared in ^{18}O-labeled water. Solid Mn oxides in the form of buserite were prepared as described previously (Mandernack et al., 1995). Sodium nitrite and sodium nitrate solutions (10 mM) were prepared in milliQ water and sterilized by autoclaving. Solutions of ^{18}O-labeled nitrite were prepared by equilibrating solutions of autoclaved nitrite in ^{18}O-labeled water in a 50 °C oven for 7 days (Buchwald and Casciotti, 2013). All experiments were initiated in 160 mL serum bottles by the addition of 1 mL of 10 mM nitrite to 100 mL of ~1 mM Mn(III)-PP in excess

pyrophosphate, giving a starting nitrite concentration of ~100 μM. Subsamples were collected over time by removing 3 mL of solution with a sterile syringe and replacing the headspace with air or N_2 gas depending on the experimental treatment. The presence of Mn(III)-PP complex was found to interfere with nitrite and nitrate concentration measurements and was thus removed prior to analysis by precipitation of all Mn as Mn oxides by the addition of 10 μL of 6 M NaOH, followed by filtration of Mn precipitate (0.2 μm) and neutralization by addition of HCl.

2.3. Chemical speciation

Concentrations of nitrate plus nitrite were measured using chemiluminescent NO_x detection (Teledyne, T200) after reduction in hot acidic vanadyl sulfate solution (Braman and Hendrix, 1989). Nitrite concentrations were monitored using Griess reagent (Pai et al., 1990), and nitrate concentration estimated by difference. Samples were diluted 10-fold with milliQ water to a final volume of 3 mL, treated with 60 μL sulfanilamide (SAN) and 60 μL *N*-(1-Naphthyl)ethylenediamine (NED) and measured for absorbance at 543 nm. Mn(III) concentrations were measured using the leucoberbelin blue method referenced to a standard curve of potassium permanganate and adjusted to account for the oxidation state offset (Jones et al., 2019; Krumbein and Altman, 1973).

2.4. Isotopic measurements

Isotopic ratios ($^{15}N/^{14}N$, $^{18}O/^{16}O$) are reported using standard delta notation where $\delta^{15}N = [(^{15}R_{sample}/^{15}R_{N2\text{-}ATM}) - 1) * 1000]$ and $^{15}R = {}^{15}N/^{14}N$ and where $\delta^{18}O = [(^{18}R_{sample}/^{18}R_{VSMOW}) - 1) * 1000]$ and $^{18}R = {}^{18}O/^{16}O$. Isotopic composition of nitrite was measured after conversion of 20–30 nmol to nitrous oxide (N_2O) using the azide method (McIlvin and Altabet, 2005) in 20 mL crimp-sealed headspace vials. Nitrate N and O isotopes were measured using the denitrifier method (Casciotti et al., 2002; Sigman et al., 2001) to convert samples to nitrous oxide after removal of nitrite by sulfamic acid addition (Granger and Sigman, 2009). The resulting N_2O was then purified and trapped on a modified TraceGas (IsoPrime, Inc.) purge and trap system coupled with a Gilson autosampler before isotopic analysis on an isotope ratio mass spectrometer (IRMS) (IsoPrime 100, Elementar Inc.). Isotope reference materials for nitrate (USGS 32, USGS 34, USGS 35) or nitrite (WILIS 10, WILIS 11 and WILIS 20) were run before and after samples at 3 different sizes to normalize reported isotope values and correct for variations in sample size and any instrument drift. Values of USGS 32, USGS 34, and USGS 35 are +180, −1.8, and +2.7‰ for $\delta^{15}N$ and +25.4, −27.8, and +56.8‰ for $\delta^{18}O$, respectively (Brand et al., 2009). Inter-laboratory comparisons set the values of WILIS 10, WILIS 11, and WILIS 20 at −1.7, +57.1, and −7.8‰ for $\delta^{15}N$ and +13.2, +8.6 and +47.6‰ for $\delta^{18}O$ (Wankel et al., 2017). Typical reproducibility is ±0.2‰ for both $\delta^{15}N$ and $\delta^{18}O$ using the azide method and ±0.2‰ for $\delta^{15}N$ and ±0.5‰ for $\delta^{18}O$ using the denitrifier method. Here we adopt the isotope notation convention wherein reactions resulting in products with a preference for lighter isotopes are indicated by a 'normal' isotope effect with a positive sign; thus, a negative sign indicates an inverse isotope effect.

3. RESULTS

3.1. Concentrations of nitrite and nitrate

Nitrite (100 μM) was reacted with Mn(III)-PP (~1 mM) under a headspace of air over a period of 11 days at three pH treatments (pH = 5.0, 5.7, 6.5) with four replicates. Over the course of the experiment, nitrite concentrations were monitored and found to decrease to undetectable levels (<1 μM) by the end of the experiment, with higher pH treatments reacting more slowly (Fig. 1a). At the conclusion of the experiment, concentrations of nitrate produced were 1:1 with nitrite consumed (not shown). Parallel controls without pyrophosphate or Mn(III)-PP showed no loss of nitrite during the experiment.

3.2. Isotopic fractionation

Nitrite $\delta^{15}N$ values universally decreased from their starting value during the course of the reaction in relation with the proportion of nitrite consumed ($\delta^{15}N$ of starting nitrite: −2.3‰). Oxygen isotope ratios showed no statistical difference between starting and ending values. Calculation of the N isotope effect of nitrite oxidation by Mn(III)-PP ($^{15}\varepsilon_{NO2ox,MnIII}$) assuming closed-system Rayleigh dynamics (Mariotti et al., 1981) yielded $^{15}\varepsilon_{NO2ox,MnIII}$ values of -19.1 ± 0.5‰ for pH = 5.0 ($r^2 = 0.997$) and $^{15}\varepsilon_{NO2ox,MnIII} = -18.2 \pm 0.4$‰ for pH = 5.7 ($r^2 = 0.997$) in initial experiments. Nitrogen isotope effects were also calculated during a subset of reaction kinetics experiments described below and ranged from -19.2 ± 0.4‰ to -20.6 ± 0.2‰ (Fig. 1b; Table 1).

3.3. Reaction kinetics

Two experiments were conducted in order to determine the reaction kinetics and order with respect to Mn(III)-PP and nitrite. The isolation method was used, in which initial concentration of one reagent was varied while other variables were held constant. Solutions of varying Mn(III)-PP concentration were prepared by v/v dilution of an approximately 1 mM solution with 5 mM pyrophosphate. All experiments were run with air as the headspace at pH = 5.0 (Table 1).

To determine the role of pH in the kinetics of reaction, incubations were conducted at pH = 5.0, 5.7, and 6.5. Solution pH was buffered by excess pyrophosphate with pH stability confirmed by measurement at the conclusion of the experiment. Solid oxides were added to minimize influence of Mn(III)-PP loss during the reaction (additional Mn(III)-PP complex will form in the presence of excess Mn oxides and pyrophosphate ligand). An additional control with Mn oxides and no pyrophosphate ligand displayed no reactivity with nitrite.

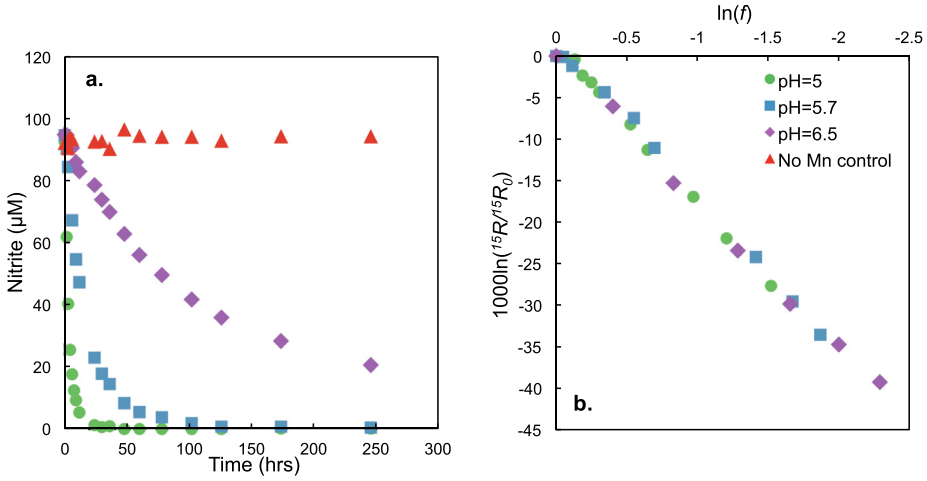

Fig. 1. Nitrite concentration vs. time (a) and closed-system Rayleigh distillation of $\delta^{15}N\text{-}NO_2^-$ (b). Data points represent the average of four replicates with standard deviations smaller than the symbols. Higher pH treatments reacted more slowly and no measureable change in nitrite was observed in a no Mn addition control. Slopes of $\ln([NO_2^-])$ vs. $\ln(^{15}R)$ were used to calculate $^{15}\varepsilon_{NXR,MnIII,}$ but are plotted here as $\ln(f)$ vs. $1000\ln(^{15}R/^{15}R_0)$.

Table 1
Summary of isotope effects for nitrite oxidation by Mn(III)-PP ($^{15}\varepsilon_{NXR,\ Mn(III)}$).

pH	Mn(III)-PP (μM)	NO_2^- (μM)	Headspace	$^{15}NO_3^-$ (μM)	$^{15}\varepsilon_{NXR,\ Mn(III)}$ (‰)		
5.0	1000	100	Air	–	−19.1	±	0.5
5.7	1000	100	Air	–	−18.2	±	0.4
5.0	1000	100	Air	–	−20.3	±	0.3
5.0	900	100	Air	–	−20.2	±	0.3
5.0	800	100	Air	–	−19.9	±	0.3
5.0	700	100	Air	–	−20.1	±	0.4
5.0	600	100	Air	–	−20.1	±	0.4
5.0	500	100	Air	–	−19.6	±	0.5
5.0	1000	50	Air	–	−19.8	±	0.3
5.0	1000	75	Air	–	−20.6	±	0.2
5.0	1000	100	Air	–	−19.6	±	0.5
5.0	1000	125	Air	–	−19.9	±	0.2
5.0	1000	150	Air	–	−20.2	±	0.2
5.0	1000	175	Air	–	−19.9	±	0.2
5.0	1000	100	N_2-purged	–	−19.8	±	0.3
5.0	1000	100	Air	–	−20.1	±	0.1
5.0	1000	100	Air	10	−19.6	±	0.6
5.0	1000	100	Air	100	−19.4	±	0.3
5.7	1000	100	Air	10	−19.2	±	0.4
5.7	1000	100	Air	100	−20.5	±	0.2

Using the balanced reaction (Eq. (1)), a general rate law (Eq. (2)) was written to derive the rate of reaction. Concentrations in Eq. (2) represent the total concentration of each reactant. For simplicity of notation, $[NO_2^-]$ also includes any nitrous acid (HNO_2) present.

$$NO_2{}^- + 2Mn(III)\text{-}PP + H_2O \rightarrow NO_3{}^- + 2Mn^{2+} + 2PP + 2H^+ \quad (1)$$

$$\frac{d[NO_3^-]}{dt} = k[Mn(III)PP]^a[NO_2^-]^b[H^+]^c \quad (2)$$

$$rate = \frac{d[NO_3^-]}{dt} = -2\frac{d[Mn(III)PP]}{dt} = -\frac{d[NO_2^-]}{dt} \quad (3)$$

where a, b, c represent the order of the reaction with respect to Mn(III)-PP, NO_2^-, and H^+, respectively, and k is the rate constant. When [Mn(III)-PP] is varied while pH and $[NO_2^-]$ held constant Eq. (2) simplifies to:

$$rate = k_{obs,1}[Mn(III)PP]^a \quad (4)$$

where

$$k_{obs,1} = k[NO_2^-]^b[H^+]^c \quad (5)$$

Using the instantaneous rate method Eq. (4) can be rewritten as:

$$\log(rate_{ins}) = \log(k_{obs,1}) + a\log([Mn(III)PP_{in}]) \quad (6)$$

where $rate_{ins}$ is the instantaneous rate and $[Mn(III)PP_{in}]$ is the initial concentration of Mn(III)-PP. Thus, the slope (a) of $\log([Mn(III)PP_{in}]$ vs. $\log(rate_{ins})$ indicated a 2nd

order reaction with respect to Mn(III)-PP ($a = 1.95 \pm 0.1$; Fig. 2a).

Similarly, when $[NO_2^-]$ is varied and [Mn(III)-PP] is held constant Eq. (2) can be written as:

$$rate = k_{obs,2}[NO_2^-]^b \quad (7)$$

with

$$k_{obs,2} = k[Mn(III)PP]^a[H^+]^c \quad (8)$$

As above this can be expressed as:

$$\log(rate_{int}) = \log(k_{obs,2}) + b\log([NO_2^-]_{in}) \quad (9)$$

The slope (b) of $\log([NO_2^-]_{in})$ vs. $\log(rate_{int})$ gave a value of 1.03 ± 0.04, indicating the reaction is 1st order with respect to NO_2^- (Fig. 2b).

To determine the role of pH, reactions were conducted in the presence of excess Mn oxides and pyrophosphate, to minimize any changes in the concentration of Mn(III)-PP. Thus, assuming constant [Mn(III)-PP], kinetics appeared pseudo-first order with respect to nitrite and rate constants were calculated from the slope of time vs. $\ln([NO_2^-])$ (Fig. 2c). As above the rate expression was simplified:

$$rate = k_{obs,3}[H^+]^c \quad (10)$$

with

$$k_{obs,3} = k[Mn(III)PP]^a[NO_2^-]^b \quad (11)$$

Using the pseudo-first order rate constants derived as described above:

$$\log(rate) = \log(k_{obs,3}) + c\log([H^+]) \quad (12)$$

Eq. (12) was solved for the slope c, indicating the reaction is 1st order with respect to concentration of protons (Fig. 2d; $c = 0.96 \pm 0.01$). The overall rate expression is thus:

$$\frac{d[NO_3^-]}{dt} = k[Mn(III)PP]^2[NO_2^-][H^+] \quad (13)$$

This rate expression can also be simplified as:

$$\frac{d[NO_3^-]}{dt} = k[Mn(III)PP]^2[HNO_2]K_a \quad (14)$$

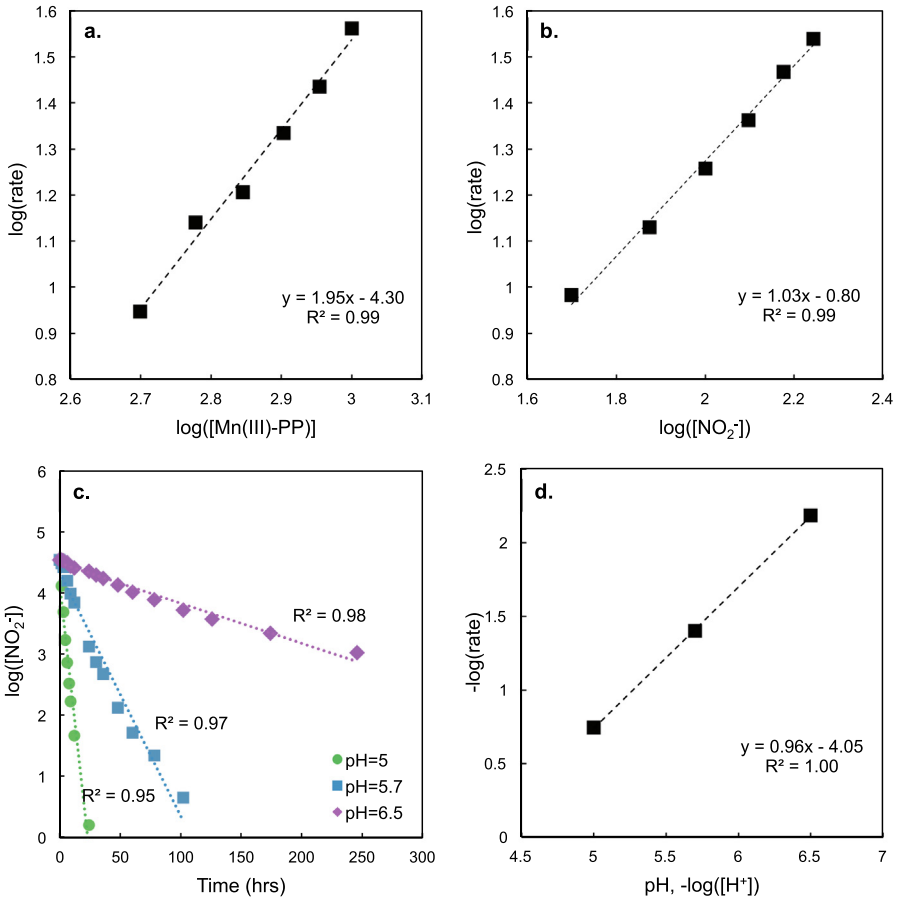

Fig. 2. Log(rate) vs. log([Mn(III)-PP] (a), $\log([NO_2^-])$ (b), and $-\log([H^+])$ (d). $\text{Log}([NO_2^-])$ vs. time (c) at pH = 5, 5.7, 6.5 in the presence of excess Mn(III)-PP displays pseudo-first order kinetics with respect to nitrite. Slope of linear regression represents the order of reaction with respect to that reactant, thus the reaction is second order in Mn(III)-PP and first order in NO_2^- and H^+.

Where K_a represents the acid dissociation constant of nitrous acid. Thus we conclude the reactant is HNO_2, rather than NO_2^-.

3.4. Reaction rates

Based on observed changes in concentrations over time for experiments at pH = 5.0, 5.7, and 6.5 (starting NO_2^- = 100 μM and Mn(III)-PP = 1000 μM, four replicates), nitrite reduction rates of 518 ± 16.8, 108 ± 4.8, and 21.6 ± 2.4 μM d^{-1} were calculated, respectively (Table 2). Additional incubation experiments were performed with the same starting concentration of Mn(III)-PP at pH 7 and 8 using isotopically labeled $^{15}NO_2^-$ to determine the reaction rates at pH values relevant to the marine system (Beman et al., 2013; Ward, 2011). Unlabeled nitrite (9 mM), ^{15}N-nitrite (1 mM), and unlabeled nitrate (4 mM) were premixed and aliquotted into bottles as described above and then sampled over 3 months to track accumulation of ^{15}N in the NO_3^- pool over time. Under these reaction conditions rates of nitrite oxidation by Mn(III)-PP at pH 7 and 8 were 5.8 ± 1.3 and 3.9 ± 0.6 μM d^{-1}, respectively (Table 2).

3.5. Effect of dissolved oxygen

To determine the potential role of oxygen in the oxidation of nitrite to nitrate by Mn(III)-PP, two parallel incubations were conducted either with a headspace of laboratory air or after vigorously purging with N_2 gas for 15 minutes to substantially reduce the amount of dissolved oxygen. Experiments were run at pH 5 and sampled over 4 days. No significant difference in reaction rates was found between the oxic and N_2-sparged treatments (Table 1, Fig. 3). Similarly, the observed N isotope fractionation was unaltered by oxygen level (p = 0.28).

3.6. Potential reversibility of reaction

To test the possibility of reaction reversibility, experiments were run with the addition of nitrate having an elevated $\delta^{15}N$ value (USGS 32, $\delta^{15}N$ = +180‰). Two treatments contained an additional 10 μM (10% of nitrite added) and 100 μM (100% of nitrite added) nitrate at the beginning of each experiment at two pH values (pH = 5.0, 5.5). Sub-samples were collected over a period of 8 days. Again, no observed change in $^{15}\varepsilon_{NO2ox,MnIII}$ was noted among treatments receiving high $\delta^{15}N$-NO_3^- in comparison to previous experiments receiving no NO_3^- amendment (Table 1).

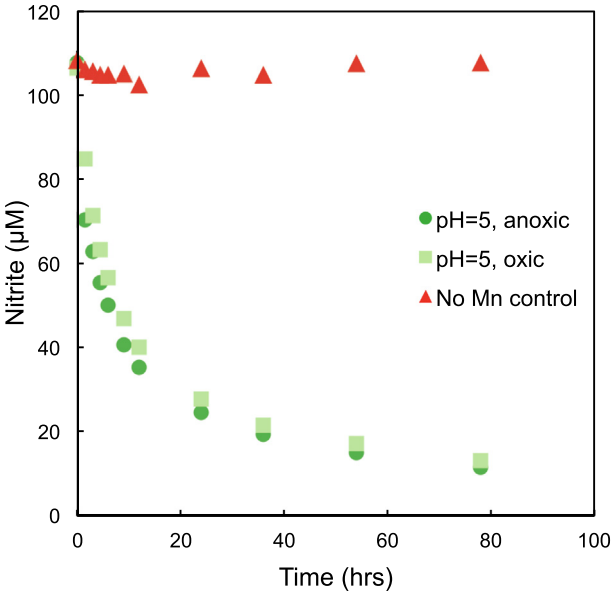

Fig. 3. Time course of nitrite concentration at pH = 5. No significant difference in rate was observed between air and N_2-purged headspace treatments. A control treatment with no Mn addition showed no significant decrease in nitrite.

3.7. Source of additional oxygen atom

In order to determine the source of the additional oxygen atom in nitrate, an experiment using ^{18}O-labeled water was performed. Two ^{18}O-labeled water samples having $\delta^{18}O$ values of approximately +18‰ and +40‰ were prepared by dilution from a stock solution (~+5000‰), with an unlabeled water sample with $\delta^{18}O \sim -5$‰ used as a third condition. As nitrite oxygen isotopes equilibrate with water quickly at the pH conditions of our experiments (Casciotti et al., 2007), ^{18}O-labeled nitrite stock solutions were also prepared as described above in an aliquot of each labeled water sample. As the result of equilibrium isotope fractionation between NO_2^- and H_2O, fully equilibrated nitrite has a $\delta^{18}O$ value ~14‰ higher than its surrounding water (Buchwald and Casciotti, 2013; Casciotti et al., 2007). Average starting values of $\delta^{18}O$-NO_2^- were +11, +32, and +54‰ after equilibration with ^{18}O-labeled water.

Five treatments ($\delta^{18}O_{water} = -5$‰, +18‰, +40‰ oxic, $\delta^{18}O = -5$‰ N_2-sparged, oxic no Mn control) were run at three pH conditions (pH = 5.0, 5.7, 6.5) and subsampled over 17 days. Samples of nitrite and nitrate were analyzed for $\delta^{18}O$. No differences in rates or $\delta^{18}O$ values were found

Table 2
Rates of nitrite oxidation and rate constants, pH = 5.0–8.0.

	Nitrite oxidation rate			Rate constant (k_{pH})		
pH	μM d^{-1}			μM^{-2} hr^{-1}		
5.0	518.4	±	16.8	2.16E−07	±	7.00E−09
5.7	108	±	4.8	4.50E−08	±	2.00E−09
6.5	21.6	±	2.4	9.00E−09	±	1.00E−09
7.0	5.8	±	1.3	2.40E−11	±	5.38E−10
8.0	3.9	±	0.6	1.62E−11	±	2.33E−10

between $\delta^{18}O\text{-}NO_3^-$ produced under oxic or N_2-sparged conditions ($p = 0.59$). The slope of $\delta^{18}O\text{-}H_2O$ vs. $\delta^{18}O\text{-}NO_3^-$ was very close to 1 under all three pH conditions, indicating water was the source of the third O-atom in nitrate (Fig. 4; Table 3). Examination of the y-intercept of these data also allows calculation of the kinetic isotope effect associated with incorporation of the O atom from water ($^{18}\varepsilon_{k,H2O}$), which was determined to be $+20.3 \pm 1.5‰$.

4. DISCUSSION

Environmental transformations of nitrogen play a fundamental role in determining its fate as a nutrient and contaminant across ecosystems. While the framework for these processes is complex, it is widely understood that microbially driven reactions comprise the large majority of these transformations. Nevertheless, there also exists an array of abiotic transformations that may contribute to the complex framework of environmental nitrogen transformations under some conditions (Doane, 2017; Heil et al., 2016; Luther, 2010; Luther et al., 2018; Zhu-Barker et al., 2015). Among these are redox reactions involving commonly abundant transition metals, especially Mn and Fe (Buchwald et al., 2016; Cavazos et al., 2018; Doane, 2017; Grabb et al., 2017; Heil et al., 2015; Stanton et al., 2018; Zhu-Barker et al., 2015). Here we demonstrate that ligand bound Mn(III) can serve as an important oxidant of nitrite, producing nitrate under environmentally relevant conditions and independent of molecular oxygen concentrations. We further present our stable isotopic interrogation of this process, shedding light on source O atoms and associated kinetic isotope effects, and discuss its possible relevance in environmental N cycling.

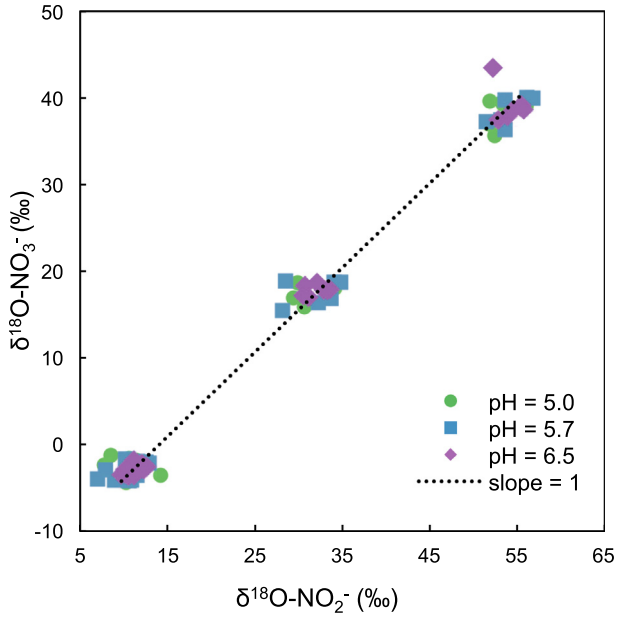

Fig. 4. $\delta^{18}O\text{-}NO_3^-$ produced from NO_2^- equilibrated with different ^{18}O-labeled H_2O samples. Slopes of best-fit lines were indistinguishable from a 1:1 line for all three pH treatments. Intercepts of the linear regressions were used for calculation of an overall kinetic isotope effect for incorporation of O from water ($^{18}\varepsilon_{k,H2O}$) as shown in Table 3.

4.1. Mn(III) is an effective oxidant of NO_2^- - with possible environmental relevance

Foremost, our results demonstrate that ligand bound Mn(III) is an effective oxidant of nitrite under the conditions evaluated including circumneutral pH and modestly elevated concentrations. While Mn is present in the environment in three oxidation states (II, III, and IV), most studies exploring the oxidative potential of oxidized Mn on the N cycle have only examined the reactivity of Mn oxide minerals, thus overlooking the possible influence of dissolved, oxidized Mn (Bartlett, 1981; Nelson et al., 2002; Stone and Morgan, 1984). Additionally, Mn oxide minerals may vary widely in structure, oxidation state, and reactivity (Post, 1999). To the best of our knowledge, the potential relevance of Mn to nitrite oxidation has only been examined in two previous studies, both involving solid-phase Mn oxides (Bartlett, 1981; Luther and Popp, 2002). Bartlett (1981) first observed abiotic oxidation of nitrite to nitrate in sterilized soils upon addition of Mn oxides, while Luther and Popp (Luther and Popp, 2002) more formally evaluated the kinetics of nitrite oxidation by colloidal Mn oxides. In contrast to these solid Mn oxide phases, ligand bound Mn(III) forms have recently been shown to comprise the majority of dissolved Mn across a range of aquatic systems (Kostka et al., 1995; Madison et al., 2011; Oldham et al., 2017a, 2015). These Mn(III)-L complexes have been shown to easily pass through conventional filtration (0.2–0.45 μm) (Kostka et al., 1995; Luther and Popp, 2002; Wilczak et al., 1993) and ultrafiltration (0.02 μm) (Oldham et al., 2017a, 2017b), suggesting that previous studies assuming that all dissolved Mn was present as Mn(II) may have overlooked an important and reactive fraction of soluble Mn. Indeed our experimental results demonstrate that Mn(III)-L complexes are viable oxidants of nitrite under conditions of environmental relevance.

4.2. Reaction rate

Over the range of conditions we evaluated, observed rates of Mn(III)-L induced nitrite oxidation ranged from 3.9 μM d^{-1} up to 518.4 μM d^{-1} over pH values from 8.0 to 5.0, respectively (Table 2). While direct comparison with other studies of nitrite oxidation by bacterial cultures or in aqueous environments is not straightforward, to a first order, our observed rates are similar to those reported in a wide variety of studies. For example, recently reported rates of aerobic nitrite oxidation by axenic cultures of nitrite-oxidizing *Nitrobacter* and *Nitrospira* bacteria yielded half saturation constants (Km) of 49–544 μM and 9–27 μM, and V_{max} values of 64–164 and 18–48 μmol mg protein^{-1} hr^{-1}, respectively (Nowka et al., 2015). Under our experimental conditions (all other factors being equal), a nitrite-oxidizer cell density corresponding to hypothetical protein concentration of 100 μg/L, would yield initial nitrite oxidation rates of 17–500 μM d^{-1} – similar in magnitude to

Table 3
Results from ^{18}O-labeled water experiments.

pH	$\delta^{18}O$-H_2O (‰)	Headspace	Slope $\delta^{18}O$ (NO_2^- vs NO_3^-)	Intercept $^{18}\varepsilon_{k,H2O}$ (‰)
5.0	−5	Air	0.95 ± 0.03 ($r^2 = 0.988$)	+20.5 ± 0.8
5.0	18	Air		
5.0	40	Air		
5.0	−5	N_2-purged		
5.7	−5	Air	0.94 ± 0.02 ($r^2 = 0.991$)	+20.2 ± 0.8
5.7	18	Air		
5.7	40	Air		
5.7	−5	N_2-purged		
6.5	−5	Air	0.97 ± 0.03 ($r^2 = 0.992$)	+22.5 ± 0.4
6.5	18	Air		
6.5	40	Air		
6.5	−5	N_2-purged		

the initial Mn(III)-L induced rates we observed at pH 5.0 and 5.7 of 518 μM d^{-1} and 108 μM d^{-1}, respectively.

Rates of nitrite oxidation in aqueous environments, of course, are much lower than those observed in bacterial cultures or lab experiments, and are therefore commonly measured by addition of $^{15}NO_2^-$ and measured accumulation of $^{15}NO_3^-$ with time (Ward, 2011). In particular, much effort has focused on characterization of nitrite oxidation rates in oxygen deficient hotspots of nitrogen transformation in the global ocean – yielding values ranging from 0 to ~600 nM d^{-1} (Beman et al., 2013; Bristow et al., 2016; Lupschultz et al., 1990; Peng et al., 2015; Sun et al., 2017; Ward et al., 1989). Other studied environments include coastal environments, open ocean, estuaries, and coral reefs, also typically exhibit rates ranging from ~0 up to several hundred nM d^{-1} (Bianchi et al., 1997; Dore and Karl, 1996; Heiss and Fulweiler, 2016). While microbial nitrite oxidation is generally considered to be an aerobic process, under oxygen-restricted conditions, the anaerobic oxidation of ammonium (anammox) is also known to oxidize NO_2^- to NO_3^- at stoichiometry of ~0.19 moles of NO_3^- produced per mole of NH_4^+ oxidized (Jetten et al., 1999; Kartal et al., 2011; Strous et al., 2006). Extrapolating from measured anammox rates in oceanic oxygen deficient zones (ODZs) and groundwaters suggests that environmental anammox based nitrite oxidation rates may range from <1 nM d^{-1} up to 70 nM d^{-1} (Dalsgaard et al., 2005; Kuypers et al., 2003; Lam et al., 2007; Moore et al., 2011).

Turning to the only previously reported rates of Mn induced nitrite oxidation, Luther and Popp (2002) reported a rate constant (k) of 493 M^{-1} min^{-1} at pH = 5.00 for reaction of NO_2^- with "polymeric" (colloidal) Mn oxides. Thus, relative to rates we observe in our experiment, at [MnO_2] = 1 mM and [NO_2^-] = 100 μM, the predicted rate of NO_3^- formation would be several orders of magnitude greater than rates we observed. Nevertheless, Mn oxides, including colloids, will be considerably lower than 1 mM in most environments, and could be less reactive due to surface adsorbates and/or co-precipitates. Further, Mn(III)-L and Mn oxides are oftentimes decoupled spatially. For instance, along redoxclines in stratified systems, Mn(III)-L span a wide redox gradient, while Mn oxides have a distinct peak in their distribution along the gradient (Dijkstra et al., 2018; Trouwborst et al., 2006; Yakushev et al., 2009, 2007). In any regards, predicted rates of nitrite oxidation by Mn(III)-L are similar in magnitude to biological rates described above. For example, under conditions that might typify porewaters close to an estuarine sediment-water interface (pH 6.5, [NO_2^-] = 10 μM, [Mn(III)-PP] = 80 μM) an estimate of 14 nM d^{-1} would be feasible (Madison et al., 2013). This result suggests that abiotic nitrite oxidation by Mn(III)-L complexes may be competitive with corresponding microbial processes, particularly at pH < 7 (Table 4). When taken together with the previously demonstrated potential for Mn oxides to also oxidize nitrite, Mn may therefore represent an important and currently underappreciated oxidant of nitrite within some ecosystems.

4.3. Stable isotope dynamics

Nitrite does not readily accumulate in most aquatic environments, with concentrations rarely reported above more than a few μM. Nevertheless, as with other reactive intermediates, its low concentrations reflect its high reactivity and fluxes involving nitrite can be high. As a consequence of these low ambient levels, nitrite has only recently been interrogated by stable isotope analyses. As both a reductive and oxidative intermediate of several

Table 4
Theoretical rates of nitrite oxidation under environmentally relevant conditions.

pH	[Mn(III)PP] μM	[NO_2^-] μM	Oxidation Rate nM d^{-1}
6.0	10	10	0.6
6.0	50	10	14.2
6.0	100	10	56.9
6.5	10	10	0.2
6.5	50	10	5.4
6.5	100	10	21.6
7.0	10	10	5.8E−04
7.0	50	10	1.4E−02
7.0	100	10	5.8E−02

transformation processes, the nitrogen and oxygen isotope dynamics of nitrite are often complex and reflect multiple processes (Buchwald and Casciotti, 2013; Buchwald et al., 2018; Casciotti, 2016; Casciotti et al., 2011). Thus, there still remains much to be learned from gaining an improved understanding of the systematics that govern its natural isotopic composition across environments in particular those with strong redox variations.

Our experiments yielded a number of insights that shed light on the nature of the reaction examined. First, abiotic nitrite oxidation by Mn(III)-PP yielded an average inverse nitrogen isotope effect ($^{15}\varepsilon_{NO2ox,MnIII}$) of -19.9 ± 0.7‰ across all experiments. No significant differences in this N isotope effect were observed between experiments, indicating that both pH ($p = 0.59$) and O_2 ($p = 0.28$) did not influence N isotopic fractionation. While inverse isotope effects are not commonly observed, it is notable that biological nitrite oxidation has also been shown to exhibit this same dynamic. In a study of *Nitrococcus mobilis*, Casciotti (2009) first demonstrated this isotope behavior, suggesting that the lower zero point energy for the transition state of the ^{14}N isotopologue over the ^{15}N isotopologue for the N-O bond forming reaction favored the net transition of ^{15}N into the product pool – thereby yielding a unique ^{15}N depletion of the reactant nitrite pool over the course of the reaction. A similar dynamic has been demonstrated with anaerobic NO_2^- oxidation by anammox bacteria (Brunner et al., 2013; Kobayashi et al., 2019). This inverse isotope effect has since been invoked to explain large differences in $\delta^{15}N$ of NO_2^- and NO_3^- in oxygen deficient zones of the oceans (up to ~40‰) (Bourbonnais et al., 2015; Casciotti and McIlvin, 2007; Gaye et al., 2013; Peters et al., 2018), and in ocean sediment porewaters reported as high as 54‰ (Buchwald et al., 2018). Thus, the nitrogen isotope signature imparted by abiotic Mn-catalyzed oxidation of NO_2^- to NO_3^- appears similar in direction and magnitude to biological nitrite oxidation. Our study falls within the range of reported biological isotope effects for nitrite oxidation (−12.8‰ to −45.3‰) (Casciotti, 2009; Kobayashi et al., 2019) with differences in magnitude likely resulting from differences in bond strengths in transition states.

Second, our results also indicate no significant variation in the observed values of $^{15}\varepsilon_{NO2ox,MnIII}$, despite substantial differences in reaction rates among experimental conditions. Additionally, our evaluation of whether the unique inverse isotope effect might be explained by chemically catalyzed isotopic equilibrium between NO_2^- and NO_3^- confirmed that no backwards isotopic transfer occurred during the reaction. Had any sort of nitrogen isotope equilibrium occurred during the reaction, in-growth of ^{15}N from labeled NO_3^- (added prior to experimental initiation) back into the reactant nitrite pool would have impacted the observed kinetic isotope effect. As such, our results suggest that the reaction proceeds in a single, irreversible step.

Third, no changes in reaction rate ($p = 0.74$) or $^{15}\varepsilon_{NO2ox,MnIII}$ ($p = 0.28$) were observed whether the reaction occurred under oxygen-saturated or oxygen-depleted (N_2-sparged) conditions, illustrating that the oxidation of nitrite to nitrate by Mn(III)-pyrophosphate is effectively agnostic to oxygen and occurs under hypoxic conditions. A similar observation was also previously reported during soil incubations of soils and synthetic Mn oxides, in which no differences in reaction extent or stoichiometry were observed between vessels open to air and those purged with N_2 or CO_2 (Bartlett, 1981).

The $\delta^{18}O$ of the product nitrate derives from both reactant nitrite and the addition of a third O atom. Our experiments conducted in ^{18}O-labeled water reveal the origin of this O atom – clearly deriving from water. By pre-equilibrating reactant NO_2^- with waters having different $\delta^{18}O$ compositions, we observed a near 1:1 relationship between the experimental waters and the newly added oxygen (Fig. 4). Luther and Popp (2002) postulated that this additional O atom might derive from Mn oxide, due to balancing of loss of two protons in the reaction. Although the formation of Mn oxide particles was not observed in our study, transient formation of Mn oxides via Mn(III) disproportionation is possible. However, if Mn-bound oxygen (or even O_2) had been the source of the third oxygen atom, then the regression of $\delta^{18}O_{H2O}$ vs. $\delta^{18}O_{NO3}$ (Fig. 4) would yield a slope of ~0.66, as the contribution of the third additional O atom would have the same $\delta^{18}O$ value in all treatments (while the other two atoms from NO_2^- were in equilibrium with water). In all cases, the near 1:1 slope unequivocally reflects incorporation of O atoms from water during formation of nitrate.

In contrast to the behavior of N isotopes in this system, nitrite O isotopes quickly equilibrate with the ambient water oxygen isotopes at the pH of our experiments (Buchwald and Casciotti, 2013; Casciotti et al., 2007). Resulting from this rapid oxygen isotope equilibration of NO_2^- with ambient H_2O at our experimental pH conditions, no differences between starting and ending $\delta^{18}O$ of NO_2^- were observed. This complete oxygen isotope equilibration between nitrite and water allows us to determine the isotope effect associated with the incorporation of hydration shell water-oxygen into nitrate. Following derivations by Buchwald and Casciotti (2010), we calculate an overall kinetic isotope effect for incorporation of O from water $^{18}\varepsilon_{k,H2O} = +20.3 \pm 1.5$‰. As with the inverse N isotope effect, the isotope effect associated with incorporation of an O atom from water during Mn(III)-induced nitrite oxidation to nitrate is also analogous to the comparable isotope effect observed in nitrite oxidizing bacteria of +12.8 to +18.2‰ (Buchwald and Casciotti, 2010; Hollocher, 1984). Thus, abiotic NO_2^- oxidation by Mn(III) could conceivably operate in parallel to biological nitrite oxidation with no impact on the expected isotope dynamics of reactant NO_2^- or product NO_3^-.

4.4. Coupling of Mn and N cycling in the environment

Despite the favorable thermodynamic conditions for reactions coupling Mn and N transformations, and the commonly overlapping zonation of Mn and N species in redox transition regimes, direct evidence for the occurrence of these reactions in the environment remains limited. Coupled redox reactions between N and Mn species have been proposed by a number of previous studies using a range of

approaches (Aigle et al., 2017; Anschutz et al., 2000; Hulth et al., 1999; Lin and Taillefert, 2014; Luther and Popp, 2002; Luther et al., 1997; Mortimer et al., 2004; Thamdrup and Dalsgaard, 2000). Notably, Luther and colleagues (Luther et al., 1997, 2018; Luther, 2010) highlighted the thermodynamic favorability of reactions between Mn and N over a range of environmentally relevant conditions. Indeed, these thermodynamically favorable reactions have justified the search for microbial mediation of coupled Mn/N reactions. Studies of soils, freshwater lakes, marine sediments, and even wastewater treatment operations have variably reported either the presence or absence of evidence for redox interactions of Mn and N (Anschutz et al., 2000; Bartlett et al., 2007; Dhakar and Burdige, 1996; Fernandes et al., 2015; Heil et al., 2015; Hulth et al., 1999; Lin and Taillefert, 2014; Luther et al., 1997; Mortimer et al., 2002; Swathi et al., 2017; Thamdrup and Dalsgaard, 2000). Nevertheless, while the apparent energetic yields of many Mn/N redox couples would appear to easily support microbial metabolisms, little evidence exists implicating any direct involvement in support of metabolic energy conservation.

Our data provide some intriguing insight into possible environmental links, specifically that soluble Mn(III)-ligands may readily oxidize NO_2^- to NO_3^- – an abiotic analog of the second step in bacterial nitrification – without the notable requirement of molecular oxygen. Indeed, several studies have concluded that so-called 'anoxic nitrification' may be important in marine and estuarine sediments (Anschutz et al., 2000; Bartlett et al., 2008; Hulth et al., 1999; Luther et al., 1997; Mortimer et al., 2004, 2002), with at least one study providing evidence for Mn-linked abiotic nitrification in soils (Bartlett, 1981). If important, anoxic nitrification could provide an important link and N loss term without a requirement of molecular oxygen. Most N loss (as N_2) in soils and aquatic sediments is attributed to denitrification or anaerobic ammonium oxidation (anammox), both proceeding under low O_2 conditions and requiring oxidized forms of N as electron acceptors (e.g., NO_3^- or NO_2^-). In general, production and delivery of these electron acceptors is linked to the activity of aerobic nitrifying organisms. Hence, a process by which N is oxidized in the absence of molecular oxygen could represent an important shunt in the N cycle.

A number of previous studies have highlighted the apparent occurrence of oxidative nitrogen cycling under anoxic conditions – with associated implications for involvement of Mn (Lin and Taillefert, 2014; Luther et al., 1997). For example, several studies examining highly resolved porewater profiles noted accumulation of NO_3^- at depths below what would be expected from diffusion alone, speculating that Mn oxides must play a role as environmental oxidant of reduced N in the absence of dissolved oxygen (Anschutz et al., 2000; Bartlett et al., 2008; Hulth et al., 2005; Mortimer et al., 2004). Other studies have used experimental amendments in sediment incubations of marine sediments – specifically, looking for responses of systemic nitrogen cycling to increased availability of Mn oxides – mostly focused on reactivity of solid phase Mn (III/IV) oxides (Bartlett et al., 2007; Lin and Taillefert, 2014). Accumulation of NO_3^- and/or NO_2^- has been reported from anoxic lab incubations of Mn-rich surface sediments and sediments amended with various Mn oxides (Bartlett et al., 2007; Hulth et al., 1999). While it was suggested that differences in Mn mineral structure (e.g., phase, defects, composition, see Luther et al., 2018) could underlie variability among different environmental systems in results, it is unclear whether products of Mn reduction, which could include Mn(III)-ligand bound forms, may have played a role in the observed dynamics.

Interestingly, evidence for the oxidative 'recycling' of NO_2^- back to NO_3^- in low oxygen systems has been mounting, in both marine and terrestrial systems (Casciotti, 2016; Granger and Wankel, 2016). In low oxygen marine systems, including oxygen deficient zones (ODZs) and porewaters, nitrate N and O isotope data have consistently required substantial re-oxidative fluxes of NO_2^- to NO_3^-, albeit under low O_2 conditions (Buchwald et al., 2018; Casciotti and McIlvin, 2007; Gaye et al., 2013; Sigman et al., 2005). The mechanism of this apparently large back-flux has remained enigmatic. Intriguingly, ^{15}N-label rate measurements of nitrite oxidation in these systems have also indicated nitrite oxidation under very low O_2 (Babbin et al., 2020; Beman et al., 2013; Füssel et al., 2012; Sun et al., 2017), although some preservation approaches may induce potential artifacts (Ostrom et al., 2016). In parallel to these observational studies, multi-process multi-isotope modeling studies have also consistently concluded that substantial conversion of NO_2^- to NO_3^- under anoxic conditions is needed to explain dynamics observed in redox transition zones of ODZs, marine porewaters, and groundwater (Buchwald et al., 2018; Casciotti, 2016; Granger and Wankel, 2016). While our data cannot directly implicate the occurrence of abiotic N transformations in the environment, it is intriguing to consider the possible role of Mn (III)-L in driving some of this purported NO_2^- oxidation under low oxygen conditions. In freshwater systems, where pH is often < 7 and levels of dissolved metals are elevated, a possible role for Mn-based NO_2^- oxidation seems particularly feasible. In the absence of O_2, this mechanism provides an abiotic avenue for active NO_2^- reoxidation – promoting coupled biotic/abiotic cycling between NO_3^- and NO_2^- as suggested by modeling studies (Granger and Wankel, 2016). Reports of anoxic nitrification in soils and sediments may also reflect such a unique biotic/abiotic coupling. In comparison, marine redox transition zones exhibit higher pH and lower levels of dissolved metals (Kondo and Moffett, 2015; Landing and Bruland, 1987; Lewis and Landing, 1991; Lewis and Luther, 2000; Moffett et al., 2007; Nameroff et al., 2002). Under these conditions, oxidation of NO_2^- by Mn(III)-L is likely to be much slower. Speciation of Mn (including Mn(III)) in ODZs has not been widely examined, with only a few studies examining coincident N cycling features. Notably, Mn(III) was implicated as a controlling factor in fluxes of phosphorus within the redoxcline of the Black Sea through formation of Mn (III)-pyrophosphate complexes with proposed concentrations of ca. 50 nM within the suboxic zone (Dijkstra et al., 2018). Additionally Trouwborst et al. (2006) reported Mn(III)-L concentrations in the Black Sea up to 5 μM. Interestingly, reported maxima in dissolved Mn in the

Arabian Sea ODZ were always highly correlated with secondary nitrite maxima (Lewis and Luther, 2000) – a zone coinciding with active NO_2^- turnover in the absence of oxygen (Beman et al., 2013; Füssel et al., 2012; Sun et al., 2017). Future examination of such interactions seems duly warranted.

5. SUMMARY

We demonstrate that a Mn(III)-L complex can facilitate abiotic NO_2^- oxidation under a wide range of environment conditions relevant to freshwater, marine, and sedimentary environments. We characterized the kinetics and N- and O-stable isotope systematics of Mn(III)-PP reaction with nitrite. The overall reaction is second order with respect to Mn(III)-PP, and first order with respect to both nitrite and H^+. An inverse nitrogen isotope effect of $-19.9 \pm 0.7‰$ was observed between the product nitrate and the reactant nitrite. While inverse isotope effects such as the one we measured here are not common in kinetically-controlled reactions, it is similar in direction and magnitude to its biological analog in nitrification. The overall similarity in reaction rates and stable isotope effects of nitrite oxidation by Mn(III)-L complexes and by biologically-mediated nitrification demands further consideration of the relative importance of abiotic processes involving Mn(III)-L complexes in local nitrogen cycling.

Intriguingly, Mn(III)-PP oxidation of NO_2^- is insensitive to O_2 levels, occurring under functionally anoxic conditions (e.g., no detectable O_2) and raising the possibility of an abiotic analog to nitrification under oxygen-depleted conditions. Although Mn has long been implicated as an important player in suboxic and anoxic redox transformations, the consideration of Mn(III)-L complexes offers an additional avenue of inquiry that provides a greater mechanistic understanding for N-redox cycling in functionally anoxic environments and environments in which redox gradients facilitate interactions between Mn- and N- species of intermediate valence. Although Mn(III)-L complexes are widespread in natural waters, there is very little known about the diversity of Mn-binding ligands, including their composition, origin, and binding strength. These are all critical factors in ultimately determining the environmental conditions under which Mn(III)-L complexes facilitate N redox reactions. In any case, interactions between Mn(III)-L complexes and nitrite are a potentially critical missing link in understanding local nitrogen budgets, the ultimate fate of these two important electron acceptors, and the energetic limits of life in the absence of oxygen.

Declaration of Competing Interest

The authors declare that they have no known competing financial interests or personal relationships that could have appeared to influence the work reported in this paper.

ACKNOWLEDGMENTS

This work was supported by NSF Geobiology and Low-Temperature Geochemistry grant EAR1826940 to SDW and CMH and by NASA Earth and Space Science Fellowship NNX15AR62H to KMS. This research was further supported in part by Hanse-Wissenschaftskolleg - Institute of Advanced Studies fellowships to SDW and CMH. We are also especially thankful for the lab assistance of Dr. Chawalit "Net" Charoenpong during early development of experiments and for insightful discussions with Dr. Veronique Oldham.

APPENDIX A. SUPPLEMENTARY MATERIAL

Supplementary data to this article can be found online at https://doi.org/10.1016/j.gca.2020.11.004.

REFERENCES

Aigle A., Bonin P., Iobbi-Nivol C., Mejean V. and Michotey V. (2017) Physiological and transcriptional approaches reveal connection between nitrogen and manganese cycles in Shewanella algae C6G3. *Sci. Rep.* **7**, 44725.

Anschutz P., Sundby B., Lefrancois L., Luther, III, G. W. and Mucci A. (2000) Interactions between metal oxides and species of nitrogen and iodine in bioturbated marine sediments. *Geochim. Cosmochim. Acta* **64**, 2751–2763.

Babbin A. R., Buchwald C., Morel F. M. M., Wankel S. D. and Ward B. B. (2020) Nitrite oxidation exceeds reduction and fixed nitrogen loss in anoxic Pacific waters. *Mar. Chem.* **224**. https://doi.org/10.1016/j.marchem.2020.103814.

Bartlett R., Mortimer R. J. and Morris K. M. (2007) The biogeochemistry of a manganese-rich Scottish sea loch: Implications for the study of anoxic nitrification. *Cont. Shelf Res.* **27**, 1501–1509.

Bartlett R., Mortimer R. J. G. and Morris K. (2008) Anoxic nitrification: Evidence from Humber Estuary sediments (UK). *Chem. Geol.* **250**, 29–39.

Bartlett R. J. (1981) Nonmicrobial nitrite-to-nitrate transformation in soils. *Soil Sci. Soc. Am. J.* **45**, 1054–1058.

Beman J. M., Shih J. L. and Popp B. N. (2013) Nitrite oxidation in the upper water column and oxygen minimum zone of the eastern tropical North Pacific Ocean. *ISME J.* **7**, 2192–2205.

Bianchi M., Feliatra F., Treguer P., Vincendeau M.-A. and Morvan J. (1997) Nitrification rates, ammonium and nitrate distribution in upper layer of the water column and in sediments of the Inidian sector of the Southern Ocean. *Deep Sea Res. Part II* **44**, 1017–1032.

Bourbonnais A., Altabet M. A., Charoenpong C., Larkum J., Hu H., Bange H. W. and Stramma L. (2015) N-loss isotope effects in the Peru oxygen minimum zone studied using a mesoscale eddy as a natural tracer experiment. *Global Biogeochem. Cycles* **29**, 793–811.

Braman R. S. and Hendrix S. A. (1989) Nanogram nitrite and nitrate determination in environmental and biological materials by vanadium (III) reduction with chemiluminescence detection. *Anal. Chem.* **61**, 2715–2718.

Brand W. A., Coplen T. B., Aerts-Bijma A. T., Böhlke J. K., Gehre M., Geilmann H., Gröning M., Jansen H. G., Meijer H. A. J., Mroczkowski S. J., Qi H., Soergel K., Stuart-Williams H., Weise S. M. and Werner R. A. (2009) Comprehensive inter-laboratory calibration of reference materials for $\delta^{18}O$ versus VSMOW using various on-line high-temperature conversion techniques. *Rapid Commun. Mass Spectrom.* **23**, 999–1019.

Bristow L. A., Dalsgaard T., Tiano L., Mills D. B., Baertagnolli A. D., Wright J. J., Hallam S. J., Ulloa O., Canfield D. E., Revsbech N. P. and Thamdrup B. (2016) Ammonium and nitrite oxidation at nanomolar oxygen concentrations in oxygen minimum zone waters. *Proc. Natl. Acad. Sci.* **113**, 10601–10606.

Brunner B., Contreras S., Lehmann M. F., Matantseva O., Rollog M., Kalvelage T., Klock G., Lavik G., Jetten M. S. M., Kartal B. and Kuypers M. M. (2013) Nitrogen isotope effects induced by anammox bacteria. *Proc. Natl. Acad. Sci.* **110**, 18994–18999.

Buchwald C. and Casciotti K. L. (2010) Oxygen isotopic fractionation and exchange during bacterial nitrite oxidation. *Limnol. Oceanogr.* **55**, 1064–1074.

Buchwald C. and Casciotti K. L. (2013) Isotopic ratios of nitrite as tracers of the sources and age of oceanic nitrite. *Nat. Geosci.* **6**, 309–313.

Buchwald C., Grabb K. C., Hansel C. M. and Wankel S. D. (2016) Constraining the role of iron in environmental nitrogen transformations: Dual stable isotope systematics of abiotic NO_2^- reduction by Fe(II) and its production of N_2O. *Geochim. Cosmochim. Acta* **186**, 1–12.

Buchwald C., Homola K., Spivack A. J., Estes E. R., Murray R. W. and Wankel S. D. (2018) Isotopic constraints on nitrogen transformation rates in the deep sedimentary marine biosphere. *Global Biogeochem. Cycles* **32**, 1688–1702.

Burgin A. J., Yang W. H., Hamilton S. K. and Silver W. L. (2011) Beyond carbon and nitrogen: how the microbial energy economy couples elemental cycles in diverse ecosystems. *Front. Ecol. Environ.* **9**, 44–52.

Casciotti K. L. (2009) Inverse kinetic isotope fractionation during bacterial nitrite oxidation. *Geochim. Cosmochim. Acta* **73**, 2061–2076.

Casciotti K. L. (2016) Nitrogen and Oxygen Isotopic Studies of the Marine Nitrogen Cycle. *Ann. Rev. Mar. Sci.* **8**, 379–407.

Casciotti K. L., Böhlke J. K., McIlvin M., Mroczkowski S. and Hannon J. (2007) Oxygen isotopes in nitrite: Analysis, calibration and equilibration. *Anal. Chem.* **79**, 2427–2436.

Casciotti K. L., Buchwald C., Santoro A. E. and Frame C. (2011) *Assessment of Nitrogen and Oxygen Isotopic Fractionation During Nitrification and Its Expression in the Marine Environment, Methods in Enzymology*. Elsevier.

Casciotti K. L. and McIlvin M. R. (2007) Isotopic analyses of nitrate and nitrite from reference mixtures and application to Eastern Tropical North Pacific waters. *Mar. Chem.* **107**, 184–201.

Casciotti K. L., Sigman D. M., Galanter-Hastings M., Böhlke J. K. and Hilkert A. (2002) Measurement of the oxygen isotopic composition of nitrate in seawater and freshwater using the denitrifier method. *Anal. Chem.* **74**, 4905–4912.

Cavazos A. R., Taillefert M., Tang Y. and Glass J. B. (2018) Kinetics of nitrous oxide production from hydroxylamine oxidation by birnessite. *Mar. Chem.* **202**, 49–57.

Dalsgaard T., Thamdrup B. and Canfield D. E. (2005) Anaerobic ammonium oxidation (anammox) in the marine environment. *Res. Microbiol.* **156**, 457–464.

Dhakar S. P. and Burdige D. J. (1996) A coupled, non-linear, steady-state model for early diagenesis processes in pelagic sediments. *Am. J. Sci.* **296**, 296–330.

Dijkstra N., Krall P., Seguret M., Flores M., Gonzalez S., Rijkenberg M. and Slomp C. P. (2018) Phosphorus dynamics in and below the redoxcline in the Black Sea and implications for phosphorus burial. *Geochim. Cosmochim. Acta* **222**, 685–703.

Doane T. A. (2017) The Abiotic Nitrogen Cycle. *Earth Space Chem.* **1**, 411–421.

Dore J. E. and Karl D. M. (1996) Nitrification in the euphotic zone as a source of nitrite, nitrate, and nitrous oxide at Station ALOHA. *Limnol. Oceanogr.* **41**, 1619–1628.

Fernandes S. O., Javanaud C., Aigle A., Michotey V. D., Guasco S., Deborde J., Deflandre B., Anschutz P. and Bonin P. (2015) Anaerobic nitrification-denitrification mediated by Mn-oxides in meso-tidal sediments: Implications for N_2 and N_2O production. *J. Mar. Syst.* **144**, 1–8.

Füssel J., Lam P., Lavik G., Jensen M. M., Holtappels M., Günter M. and Kuypers M. M. (2012) Nitrite oxidation in the Namibiam oxygen minimum zone. *ISME J.* **6**, 1200–1209.

Gaye B., Nagel B., Dähnke K., Rixen T. and Emeis K.-C. (2013) Evidence of parallel denitrification and nitrite oxidation in the ODZs of the Arabian Sea from paired stable isotopes of nitrate and nitrite. *Global Biogeochem. Cycles* **27**, 1059–1071.

Grabb K. C., Buchwald C., Hansel C. M. and Wankel S. D. (2017) A dual isotopic investigation of chemodenitrification by mineral-associated Fe(II) and its production of nitrous oxide. *Geochim. Cosmochim. Acta* **196**, 388–402.

Granger J. and Sigman D. M. (2009) Removal of nitrite with sulfamic acid for nitrate N and O isotope analysis with the denitrifier method. *Rapid Commun. Mass Spectrom.* **23**, 3753–3762.

Granger J. and Wankel S. D. (2016) Isotopic overprinting of nitrification on denitrification as a ubiquitous and unifying feature of environmental nitrogen cycling. *PNAS* **113**, E6391–E6400.

Gruber N. and Galloway J. N. (2008) An Earth-system perspective of the global nitrogen cycle. *Nature* **451**, 293–296.

Heil J., Liu S., Verecken H. and Brüggeman N. (2015) Abiotic nitrous oxide production from hydroxylamine in soils and their dependence on soil properties. *Siol. Biol. Biochem.* **84**, 107–115.

Heil J., Verecken H. and Brüggeman N. (2016) A review of chemical reactions of nitrification intermediates and their role in nitrogen cycling and nitrogen trace gas formation in soil. *Eur. J. Soil Sci.* **67**, 23–39.

Heiss E. M. and Fulweiler R. W. (2016) Coastal water column ammonium and nitrite oxidation are decoupled in summer. *Estuar. Coast. Shelf Sci.* **178**, 110–119.

Hollocher T. C. (1984) Source of the Oxygen Atoms of Nitrate in the Oxidation of Nitrite by *Nitrobacter agilis* and Evidence against a P-O-N Anhydride Mechanism in Oxidative Phosphorylation. *Arch. Biochem. Biophys.* **233**, 721–727.

Hulth S., Aller R. C., Canfield D. E., Dalsgaard T., Engström P., Gilbert F., Sundbäck K. and Thamdrup B. (2005) Nitrogen removal in marine environments: Recent findings and future research challenges. *Mar. Chem.* **94**, 125–145.

Hulth S., Aller R. C. and Gilbert F. (1999) Coupled anoxic nitrification/manganese reduction in marine sediments. *Geochim. Cosmochim. Acta* **63**, 49–66.

Jetten M. S., Strous M., van de Pas-Schoonen K. T., Schalk J., van Dongen U. G., van de Graaf A. A., Logemann S., Muyzer G., van Loosdrecht M. C. and Kuenen J. G. (1999) The anaerobic oxidation of ammonium. *FEMS Microbiol. Rev.* **22**, 421–437.

Jones M. R., Luther G. W., Mucci A. and Tebo B. M. (2019) Concentrations of reactive Mn(III)-L and MnO2 in estuarine and marine waters determined using spectrophotometry and the leuco base, leucoberbelin blue. *Talanta* **200**, 91–99.

Kartal B., Maalcke W. J., de Almeida N. M., Cirpus I., Gloerich J., Geerts W., Op den Camp H. J., Harhangi H. R., Janssen-Megens E. M., Francoijs K.-J., Stunnenberg H. G., Keltjens J. T., Jetten M. S. and Strous M. (2011) Molecular mechanims of anaerobic ammonium oxidation. *Nature* **479**, 127–130.

Kendall C., Elliott E. M. and Wankel S. D. (2007) Tracing anthropogenic inputs of nitrogen to ecosystems. In *Stable Isotopes in Ecology and Environmental Science* (eds. R. H. Michener and K. Lajtha), second ed. Blackwell Publishing, p. 592.

Kobayashi K., Makabe A., Yano M., Oshiki M., Kindaichi T., Casciotti K. L. and Okabe S. (2019) Dual nitrogen and oxygen isotope fractionation during anaerobic ammonium oxidation by anammox bacteria. *ISME J.*.

Kondo Y. and Moffett J. W. (2015) Iron redox cycling and subsurface offshore transport in the eastern tropical South Pacific oxygen minimum zone. *Mar. Chem.* **168**, 95–103.

Kostka J. E., Luther, III, G. W. and Nealson K. H. (1995) Chemical and biological reduction of Mn(III)-pyrophosphate complexes: Potential importance of dissolved Mn(III) as an environmental oxidant. *Geochim. Cosmochim. Acta* **59**, 885–894.

Krumbein W. E. and Altman H. J. (1973) A new method for detection and enumeration of manganese-oxidizing and -reducing microorganisms. *Helgol. Wiss. Meeresunters* **25**, 347–356.

Kuypers M. M. M., Sliekers A. O., Lavik G., Schmid M., Jorgensen B. B., Kuenen J. G., Damste J. S. S., Strous M. and Jetten M. S. M. (2003) Anaerobic ammonium oxidation by anammox bacteria in the Black Sea. *Nature* **422**, 608–610.

Lam P., Jensen M. M., Lavik G., McGinnis D. F., Muller B., Schubert C. J., Amann R., Thamdrup B. and Kuypers M. M. M. (2007) Linking crenarchaeal and bacterial nitrification to anammox in the Black Sea. *PNAS* **104**, 7104–7109.

Landing W. M. and Bruland K. W. (1987) The contrasting biogeochemistry of iron and manganese in the Pacific Ocean. *Geochim. Cosmochim. Acta* **51**, 29–43.

Lewis B. L. and Landing W. M. (1991) The biogeochemistry of manganese and iron in the Black Sea. *Deep Sea Res. Part A – Oceanogr. Res. Papers* **38**, S773–S803.

Lewis B. L. and Luther, III, G. W. (2000) Processes controlling the distribution and cycling of manganese in the oxygen minimum zone of the Arabian Sea. *Deep Sea Res. Part II* **47**, 1541–1561.

Lin H. and Taillefert M. (2014) Key geochemical factors regulating Mn(IV)-catalyzed anaerobic nitrification in coastal sediments. *Geochim. Cosmochim. Acta* **133**, 17–33.

Lupschultz F., Wofsy S. C., Ward B. B., Codispoti L. A., Friedrich G. and Elkins J. (1990) Bacterial transformations of inorganic nitrogen in the oxygen-deficient waters of the Eastern Tropical South Pacific Ocean. *Deep-Sea Res.* **37**, 1513–1541.

Luther, III, G. W. and Popp J. I. (2002) Kinetics of the abiotic reduction of polymeric manganese dioxide by nitrite: An anaerobic nitrification reaction. *Aquat. Geochem.* **8**, 15–36.

Luther, III, G. W., Sundby B., Lewis B. L., Brendel P. J. and Silverberg N. (1997) Interactions of manganese with the nitrogen cycle: Alternative pathways to dinitrogen. *Geochim. Cosmochim. Acta* **61**, 4043–4052.

Luther, III, G. W. (2010) The role of one- and two-electron transfer reactions in forming thermodynamically unstable intermediates as barriers in multi-electron redox reactions. *Aquat. Geochem.* **16**, 395–420.

Luther G. W., Thibault de Chanvalon A., Oldham V. E., Estes E. R., Tebo B. M. and Madison A. S. (2018) Reduction of Manganese Oxides: Thermodynamic, Kinetic and Mechanistic Considerations for One- Versus Two-Electron Transfer Steps. *Aquat. Geochem.* **24**, 257–277.

Madison A. S., Tebo B. M. and Luther, III, G. W. (2011) Simultaneous determination of soluble manganse(III), manganese(II) and total manganese in natural (pore)waters. *Talanta* **84**, 374–381.

Madison A. S., Tebo B. M., Mucci A., Sundby B. and Luther, III, G. W. (2013) Abundant porewater Mn(III) is a major component of the sedimentary redox system. *Science* **341**, 875–878.

Mandernack K. W., Fogel M. L., Tebo B. M. and Usui A. (1995) Oxygen isotope analyses of chemically and microbially produced manganese oxides and manganates. *Geochim. Cosmochim. Acta* **59**, 4409–4425.

Mariotti A., Germon J. C., Hubert P., Kaiser P., Letolle R., Tardieux A. and Tardieux P. (1981) Experimental determination of nitrogen kinetic isotope fractionation: some principles; illustration for the denitrification and nitrification processes. *Plant Soil* **62**, 413–430.

McIlvin M. and Altabet M. A. (2005) Chemical conversion of nitrate and nitrite to nitrous oxide for nitrogen and oxygen isotopic analysis in freshwater and seawater. *Anal. Chem.* **77**, 5589–5595.

Melton E. D., Swanner E. D., Behrens S., Schmidt C. and Kappler A. (2014) The interplay of microbially mediate and abiotic reactions in the biogeochemical Fe cycle. *Nat. Rev. Microbiol.* **12**, 797–808.

Moffett J. W., Goepfert T. J. and Naqvi S. W. A. (2007) Reduced iron associated with secondary nitrite maxima in the Arabian Sea. *Deep Sea Res. Part II* **54**, 1341–1349.

Moore T. A., Xing Y., Lazenby B., Lynch M. D., Schiff S. L., Robertson W. D., Timlin R., Lanza S., Ryan M. C., Aravena R., Fortin D., Clark I. D. and Neufeld J. D. (2011) Prevalence of anaerobic ammonium-oxidizing bacteria in contaminated groundwater. *Environ. Sci. Technol.* **45**, 7217–7225.

Mortimer R. J., Harris S. J., Krom M. D., Freitag T. E., Prosser J. I., Barnes J., Anschutz P., Hayes P. J. and Davies I. M. (2004) Anoxic nitrification in marine sediments. *Mar. Ecol. Prog. Ser.* **276**, 37–51.

Mortimer R. J., Krom M. D., Harris S. J., Hayes P. J., Davies I. M., Davison W. and Zhang H. (2002) Evidence for suboxic nitrification in recent marine sediments. *Mar. Ecol. Prog. Ser.* **236**, 31–35.

Nameroff T., Balistrieri L. and Murray J. W. (2002) Suboxic trace metal geochemistry in the Eastern Tropical North Pacific. *Geochim. Cosmochim. Acta* **66**, 1139–1158.

Nelson Y. M., Lion L. W., Shuler M. L. and Ghiorse W. C. (2002) Effect of oxide formation mechanisms on lead adsorption by biogenic manganese (hydr)oxides, iron (hydr)oxides and their mixtures. *Environ. Sci. Technol.* **36**, 421–425.

Nowka B., Diams H. and Spieck E. (2015) Comparison of oxidation kinetics of nitrite-oxidizing bacteria: Nitrite availability as a key factor in niche differentiation. *Appl. Environ. Microbiol.* **81**, 745–753.

Oldham V. E., Jones M. R., Tebo B. M. and Luther, III, G. W. (2017a) Oxidative and reductive processes contributing to manganese cycling at oxic-anoxic interfaces. *Mar. Chem.* **195**, 122–128.

Oldham V. E., Miller M. T., Jensen L. T. and Luther, III, G. W. (2017b) Revisiting Mn and Fe removal in humic rich estuaries. *Geochim. Cosmochim. Acta* **209**, 267–283.

Oldham V. E., Owings S. M., Johnes M. R., Tebo B. M. and Luther, III, G. W. (2015) Evidence for the presence of strong Mn(III)-binding ligands in the water column of Chesapeake Bay. *Mar. Chem.* **171**, 58–66.

Ostrom N. E., Gandhi H., Trubl G. and Murray A. E. (2016) Chemodenitrification in the cryoecosystem of Lake Vida, Victoria Valley, Antarctica. *Geobiology* **14**, 575–587.

Pai S.-C., Yang C.-C. and Riley J. P. (1990) Formation kinetics of the pink azo dye in the determination of nitrite in natural waters. *Anal. Chim. Acta* **232**, 345–349.

Peng Z., Fuchsman C. A., Jayakumar A., Oleynik S., Martens-Habbena W., Devol A. H. and Ward B. B. (2015) Ammonia and nitrite oxidation in the Eastern Tropical North Pacific. *Global Biogeochem. Cycles* **29**, 2034–2049.

Peters B., Horak R., Devol A. H., Fuchsman C. A., Forbes M., Mordy C. W. and Casciotti K. L. (2018) Estimating fixen nitrogen loss and associated isotope effects using concentration and isotope measurements of NO_3^-, NO_2^-, and N_2 from the Eastern Tropical South Pacific oxygen deficient zone. *Deep-Sea Res. Part II* **156**, 121–136.

Post J. (1999) Manganese oxide minerals: Crystal structures and economic and environmental significance. *Proc. Natl. Acad. Sci. USA* **96**, 3447–3454.

Sigman D. M., Casciotti K. L., Andreani M., Barford C., Galanter M. and Böhlke J. K. (2001) A Bacterial Method for the

Nitrogen Isotopic Analysis of Nitrate in Seawater and Freshwater. *Anal. Chem.* **73**, 4145–4153.

Sigman D. M., Granger J., DiFiore P. J., Lehmann M. F., Ho R., Cane G. and van Geen A. (2005) Coupled nitrogen and oxygen isotope measurements of nitrate along the eastern North Pacific margin. *Global Biogeochem. Cycles* **19**, GB4022.

Stanton C. L., Reinhard C. T., Kasting J. F., Ostrom N. E., Haslun J. A., Lyons T. W. and Glass J. B. (2018) Nitrous oxide from chemodenitrification: A possible missing link in the Proterozoic greenhouse and the evolution of the aerobic respiration. *Geobiology*, 1–13.

Stone A. T. and Morgan J. J. (1984) Reduction and dissolution of manganese(III) and manganese(IV) oxides by organics. 2. Survey of the reactivity of organics. *Environ. Sci. Technol.* **18**, 617–624.

Strous M., Pelletier E., Mangenot S., Rattei T., Lehner A., Taylor M. W., Horn M., Diams H., Bartol-Mavel D., Winkcer P., Barbe V., Fonknechten N., Vallenet D., Segurens B., Schenowitz-Truong C., Medigue C., Collingro A., Snel B., Dutilh B. E., op den Camp H. J., van der Drift C., Cirpus I., van de Pas-Schoonen K., Harhangi H. R., van Niftrik L. A., Schmid M., Keltjens J., van de Vossenberg J., Kartal B., Meier H., Frishman D., Huynen M. A., Mewes H.-W., Weissenbach J., Jetten M. S., Wagner M. and Le Paslier D. (2006) Deciphering the evolution and metabolism of an anammox bacterium from a community genome. *Nature* **440**, 790–794.

Sun X., Ji Q., Jayakumar A. and Ward B. B. (2017) Dependence of nitrite oxidation on nitrite and oxygen in low-oxygen seawater. *Geophys. Res. Lett.* **44**, 7883–7891.

Swathi D., Sabumon P. and Maliyekkal S. (2017) Microbial mediated anoxic nitrification-denitrification in the presence of nanoscale oxides of manganese. *Int. Biodeterior. Biodegrad.* **119**, 499–510.

Thamdrup B. and Dalsgaard T. (2000) The fate of ammonium in anoxic manganese oxide-rich marine sediment. *Geochim. Cosmochim. Acta* **64**, 4157–4164.

Trouwborst R. E., Clement B. G., Tebo B. M., Glazer B. T. and Luther G. W. (2006) Soluble Mn(III) in suboxic zones. *Science* **313**, 1955–1957.

Wankel S. D., Ziebis W., Buchwald C., Charoenpong C., de Beer D., Dentinger J., Xu Z. and Zengler K. (2017) Evidence for non-traditional N_2O formation pathways in nitrogen-impacted coastal ecosystems: fungal and chemodentrification. *Nat. Commun.* **8**, 15595.

Ward B. B. (2011) Measurement and distribution of nitrification rates in the oceans. *Methods Enzymol.* **486**, 307–323.

Ward B. B., Kilpatrick K. A., Renger E. H. and Eppley R. W. (1989) Biological nitrogen cycling in the nitracline. *Limnol. Oceanogr.* **34**, 493–513.

Wilczak A., Aieta E., Knocke W. and Hubel R. (1993) Manganese control during ozonation of water containing organic compounds. *J. Am. Water Works Assoc.* **85**, 10.

Yakushev E., Pakhomova S., Sorensen K. and Skei J. (2009) Importance of the different manganese species in the formation of water column redox zones: observations and modeling. *Mar. Chem.* **117**, 59–70.

Yakushev E., Pollehne F., Jost F., Kuznetsov I., Schneider B. and Umlauf L. (2007) Analysis of the water column oxic/anoxic interface in the Black and Baltic seas with a numerical model. *Mar. Chem.* **107**, 388–410.

Zhu-Barker X., Cavazos A. R., Ostrom N. E., Horwath W. R. and Glass J. B. (2015) The importance of abiotic reactions for nitrous oxide production. *Biogeochemistry* **126**, 251–267.

Associate editor: Filip Meysman